
Rank-1 LoRAs Encode Interpretable Reasoning Signals

Jake Ward
MATS
jakenicholasward@gmail.com

Paul Riechers[†]
Simplex

Adam Shai[†]
Simplex

Abstract

Reasoning models leverage inference-time compute to significantly enhance the performance of language models on difficult logical tasks, and have become a dominating paradigm in frontier LLMs. Despite their wide adoption, the mechanisms underpinning the enhanced performance of these reasoning models are not well understood. In this work, we show that the majority of new capabilities in reasoning models can be elicited by small, single-rank changes to base model parameters, with many of these changes being interpretable. Specifically, we use a rank-1 LoRA to create a minimal parameter adapter for Qwen-2.5-32B-Instruct which recovers 73-90% of reasoning-benchmark performance compared to a full-parameter finetune. We find that the activations of this LoRA are as interpretable as MLP neurons, and fire for reasoning-specific behaviors. Finally, we train a sparse autoencoder on the entire activation state of this LoRA and identify fine-grained and monosemantic features. Our findings highlight that reasoning performance can arise largely from minimal changes to base model parameters, and explore what these changes affect. More broadly, our work shows that parameter-efficient training methods can be used as a targeted lens for uncovering fundamental insights about language model behavior and dynamics.

1 Introduction

Current frontier LLMs increasingly rely on chain-of-thought (CoT) reasoning to achieve strong performance on logical tasks [1, 7, 14]. Despite their ubiquity, we still lack a crisp, white-box understanding of the mechanisms inside the network which enable these gains. Some attempts have been made to mechanistically interpret fully finetuned reasoning models [2, 12, 13]. However, reasoning model interpretation presents a fundamental challenge: the parameters responsible for new reasoning behaviors in a finetuned model are many and differences are diffuse [11]. In this paper, we introduce an alternative approach: we use parameter-efficient methods to explicitly enforce that differences between base and finetuned models in parameter space are minimal, allowing us to perform focused and targeted interpretability experiments.

We show that a rank-1 LoRA [6] trained to adapt all layers of Qwen-2.5-32B-Instruct on a dataset of DeepSeek R1 rollouts is enough to recover 73-90% of the performance gap on reasoning benchmarks, compared to a full-parameter finetune (Table 1).

We directly interpret the directions defined by this LoRA. Because each adapted matrix is rank-1, activations of each adapter component can be represented by a single scalar. In total, our LoRA encodes 192 MLP and 256 attention adapter components across model layers and weight matrices,

[†]Equal senior author contribution.

Code for this paper is available at <https://github.com/jnward/reasoning-lora-interp>

Benchmark	Base Qwen2.5-32B-Instruct	Rank-1 LoRA	Full Finetune	% Recovery
AIME'24 (no-figures)	0.2333	0.5000	0.6000	72.73%
MATH500	0.8340	0.9100	0.9220	86.36%
GPQA-Diamond	0.4899	0.5808	0.5909	89.90%

Table 1: Performance of base model, rank-1 LoRA, and full-parameter finetune on three reasoning benchmarks. % Recovery is the fraction of the difference in performance between the base model and full finetune which is recovered by the rank-1 LoRA.

with each adapter component providing a single activation at each token position. This allows us to treat the LoRA itself as a measurement device: we find that individual adapter directions have interpretable properties comparable to those of MLP neurons, and identify monosemantic concepts encoded by these directions. Additionally, we take the entire 448-dimensional LoRA activation state, representing the entire adapter state across MLP and attention components, and train a cross-layer SAE [8]. This SAE uncovers sparse and monosemantic features which organize into categories such as *Mathematical Operators*, *Procedural Markers*, and *Discourse and Reasoning Markers* (Figure 2). Finally, perform a component-wise ablation study, and find that MLP adapters drive the majority of this change (Figure 3).

Taken together, these results show that minimal adapters both *elicit* and *expose* reasoning signals: a rank-1 LoRA is sufficient to recover the majority of reasoning performance, and yields interpretable adapter directions.

Our contributions are as follows:

- We train and open-source a rank-1 LoRA which adapts all projection matrices in Qwen-2.5-32B-Instruct. We demonstrate that this LoRA recovers 73-90% of reasoning benchmark performance compared to a full-parameter finetune.
- We show that individual adapter activations are as monosemantic as MLP neurons, and interpret these.
- We decompose the complete LoRA activation state into interpretable and monosemantic features using a cross-layer SAE.

2 Preliminaries

LoRA training We finetune Qwen-2.5-32B-Instruct using s1k-1.1, a sample-efficient dataset of 1000 DeepSeek R1 chain-of-thought trajectories and answer attempts on diverse reasoning problems [10]. For all experiments, we train on this dataset for 5 epochs using cross-entropy loss on a single 8xH200 node. We train our LoRA to adapt all three MLP matrices at every layer (up_proj, down_proj, and gate_proj), as well as all four Q, K, V, and O attention matrices at every layer. In total, our LoRA contains less than 0.03% as many trainable parameters as the base model.

Extracting LoRA activations For every $N \times M$ adapted matrix in the base model, a rank- r LoRA encodes an $N \times r$ lora_A matrix and an $r \times M$ lora_B matrix. Because $r = 1$ for our LoRA, lora_A and lora_B are N - and M -dimensional vectors respectively. We can extract scalar activations for every LoRA component by taking the activation value between lora_A and lora_B during the forward pass, which is equivalent to the projection of lora_A onto the input activation vector to the adapted matrix.

3 LoRA Analysis

3.1 Interpreting LoRA Components

We interpret LoRA activations using two different methods: by treating individual adapter activations as probes, and separately by training an SAE on the entire 448-dimensional adapter activation vector. In both cases, we generate activations over the entire training set and extract max-activating examples with associated contexts. We then use LLM autointerpretation to generate interpretations from the

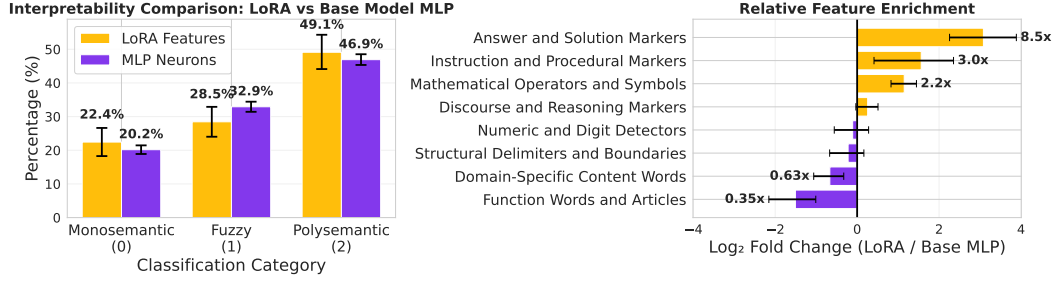
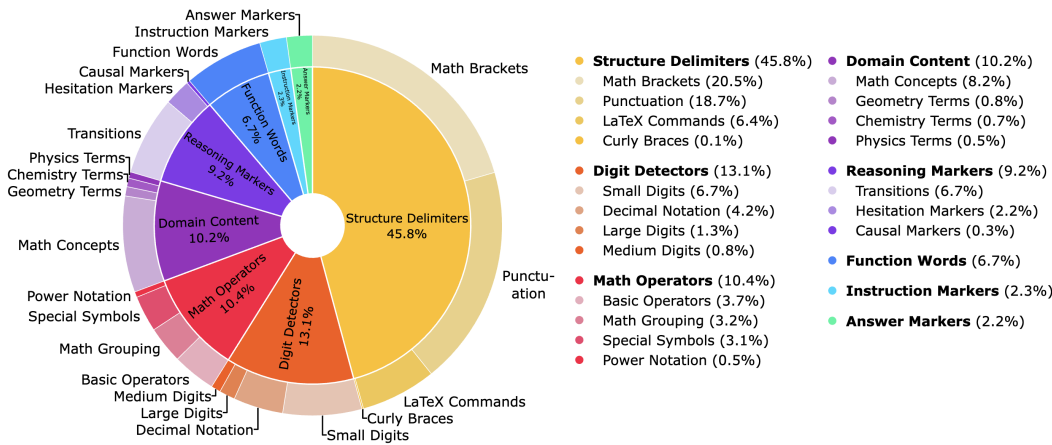


Figure 1: **(left)**: Comparison of interpretability scores of individual LoRA adapter activations to arbitrarily sampled MLP neurons, and find that LoRA activations tend to be monosemantic roughly as often. **(right)**: Comparison of autointerpretation categories between MLP neurons and LoRA adapter activations. LoRA adapters tend to activate more often for reasoning-specific feature categories.

top 64 contexts with token + activation pairs [3], use the same LLM to classify the monosemanticity of features, and finally categorize each feature such that we can compare and examine aggregate feature distributions. Categories were generated by prompting an LLM with feature interpretations and examples from an equal number of MLP neurons and LoRA directions. The exact prompts used are in Appendix B.

Direction-level interpretation We run our interpretation and feature classification pipeline both on individual LoRA activations and on the first 60 neurons of each MLP in the unadapted base model. This gives us a baseline to compare feature distributions to, allowing us to examine which feature categories the LoRA activates on compared to the baseline feature distribution in the dataset (as measured by MLP activations). We find that LoRA activations have roughly the same likelihood as MLP neurons to be monosemantic, but tend to encode different feature categories. We interpret this level of monosemanticity as a positive result for LoRA interpretation, given significant recent work utilizing MLP neurons for pragmatic interpretability tasks [5]. Relative to MLP neurons, LoRA activations are more likely to fire for text corresponding to answers or solutions, problem instructions, mathematical symbols, and reasoning discourse (Figure 1).

Cross-layer SAE over entire adapter state To gain a more fine-grained and comprehensive view of features encoded by our LoRA, we train a cross-layer sparse autoencoder (SAE) on the entire 448-dimensional LoRA activation state. We use a batch-top-k SAE with k=16, and an expansion



factor of 8 [4, 9]. After filtering for dead latents, the trained SAE contains roughly 2000 features. We run the same automated interpretation and classification pipeline on max-activating examples for each feature in this SAE, and then further categorize each feature with LLM-generated subcategories. We then visualize relative feature prevalence by computing category-wise activation densities, which is the normalized sum of feature activations within each category over a subset of training data, and plot these in figure 2. We note that this categorization methodology is subjective and sensitive to prompt verbiage, and provide this visualization only as a tool to develop high-level intuitions about the adapter’s representational budget across layers and components. Broadly, we observe that features tend to concentrate on mathematical operators and syntax, numbers, formatting tokens, and reasoning control-flow. Our LLM-based interpretability classification identifies 62% of SAE features as “cleanly monosemantic”, up from 22% of LoRA features, with an additional 22% of SAE features classified as “broad but consistent”. For a more direct look into our SAE, a selection of individual SAE feature activations and interpretations are provided in appendix A.3.

3.2 Ablation Study

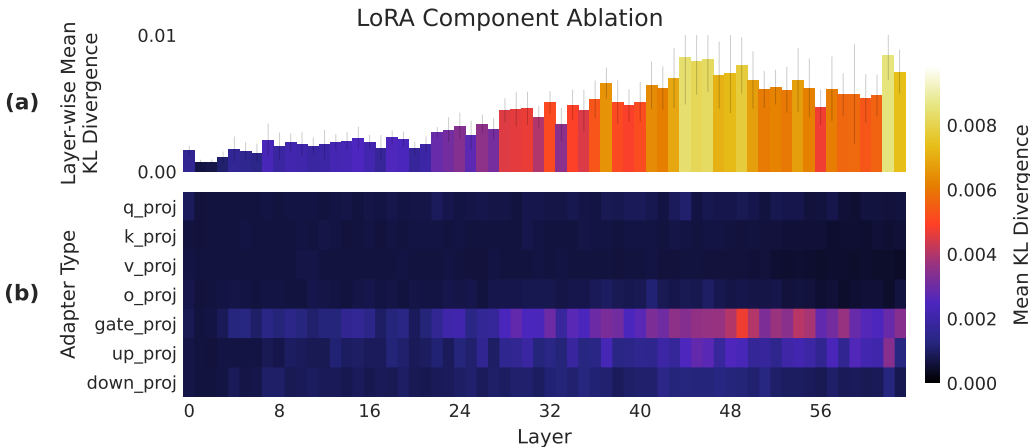


Figure 3: Effect of ablating individual LoRA components from full adapter. **(a)** Effect of ablating all adapter components at a given layer on KL divergence. **(b)** Effect of ablating each adapter component individually. Ablation at later layers tends to have a significantly greater effect on the model’s output distribution compared to earlier layers. MLP adapters, especially those trained on `gate_proj` matrices tend to have the strongest effect.

To identify which LoRA components most affect downstream performance, we conduct two ablation experiments. First, we zero out individual components and layers to measure their impact on output KL divergence relative to the unmodified LoRA. Second, we ablate all MLP components simultaneously, and separately all attention components, to assess benchmark performance impact.

Individual component ablation (Figure 3) reveals that mid-to-late layers (particularly 44, 45, 46, and 62) have the greatest effect on downstream KL. MLP components show significantly larger impact than attention components, with `gate_proj` having the strongest average effect.

Simultaneous ablation results (Table 2) confirm MLP adapters’ greater contribution: removing all attention adapters decreases performance but still outperforms the base model, while removing all MLP adapters causes severe degradation, underperforming the base model on one of three tasks and showing poor performance on the others.

4 Conclusion and Outlook

Limitations This work includes several limitations. First, we train our LoRA using a sample-efficient dataset with roughly 10 million tokens. While significant performance can be elicited using this dataset [10], it is likely that our trained models do not contain all of the circuits which are learned

by models trained on larger datasets. Additionally, we attempted to prove that extracted LoRA directions have a causal effect on model outputs when used for steering, but found inconclusive results. Anecdotally, steering experiments required very large steering magnitudes to have noticeable effects (in excess of 50x normal activation magnitudes), at which point the model would have a high propensity for backtracking (outputting the `Wait,` token, among others). More investigation of this phenomenon is required to make claims about what is going on. We also heavily use LLM-based autointerpretation and autocategorization methods in our analysis. These methods are useful for painting a general picture of model mechanisms, but we suspect they often fail to uncover the “true” role of extracted features. Finally, we only study one model, Qwen-2.5-32B-Instruct, and evaluate this model mostly on math-related reasoning benchmarks.

We demonstrate that reasoning capabilities in large language models can be substantially recovered through minimal parameter modifications, with a rank-1 LoRA recovering 73-90% of full finetuning performance while having only $\sim 0.03\%$ as many trainable parameters. Our analysis reveals that these minimal parameter changes encode interpretable, reasoning-specific signals, with individual adapter directions exhibiting monosemantic properties. Further, we find that sparse autoencoders are useful for extracting additional monosemantic features from LoRA activation states. These findings open new avenues for understanding LLMs through parameter-efficient methods, and suggest that similar targeted approaches could be useful to study other emergent capabilities. Future work could involve focused analysis identifying specific circuits that LoRAs interface with, which we hope could illuminate the core computational mechanisms underlying reasoning behavior in language models.

5 Acknowledgments

This work was completed during the ML Alignment and Theory (MATS) 8.0 program. JW thanks Elizabeth Donoway for useful discussions at the beginning of this project, and Bryce Woodworth for support throughout.

References

- [1] Openai o1 system card. Technical report, OpenAI, December 2024. URL <https://cdn.openai.com/o1-system-card-20241205.pdf>.
- [2] David D. Baek and Max Tegmark. Towards understanding distilled reasoning models: A representational approach. *arXiv preprint arXiv:2503.03730*, 2025. URL <https://arxiv.org/abs/2503.03730>. ICLR 2025 Building Trust Workshop (paper).
- [3] Steven Bills, Nick Cammarata, Dan Mossing, Henk Tillman, Leo Gao, Gabriel Goh, Ilya Sutskever, Jan Leike, Jeff Wu, and William Saunders. Language models can explain neurons in language models. <https://openaipublic.blob.core.windows.net/neuron-explainer/paper/index.html>, 2023.
- [4] Bart Bussmann, Patrick Leask, and Neel Nanda. Batchtopk sparse autoencoders. *arXiv preprint arXiv:2412.06410*, 2024. doi: 10.48550/arXiv.2412.06410. URL <https://arxiv.org/abs/2412.06410>.
- [5] Dami Choi, Vincent Huang, Kevin Meng, Daniel D. Johnson, Jacob Steinhardt, and Sarah Schwettmann. Scaling automatic neuron description. <https://transluce.org/neuron-descriptions>, October 2024. Published October 23, 2024. Accessed August 22, 2025.
- [6] Edward J. Hu, Yelong Shen, Phillip Wallis, Zeyuan Allen-Zhu, Yanzhi Li, Shean Wang, Lu Wang, and Weizhu Chen. Lora: Low-rank adaptation of large language models. *arXiv preprint arXiv:2106.09685*, 2022. URL <https://arxiv.org/abs/2106.09685>.
- [7] Takeshi Kojima, Shixiang Shane Gu, Machel Reid, Yutaka Matsuo, and Yusuke Iwasawa. Large language models are zero-shot reasoners. *arXiv preprint arXiv:2205.11916*, 2022. URL <https://arxiv.org/abs/2205.11916>.
- [8] Jack Lindsey, Adly Templeton, Jonathan Marcus, Thomas Conerly, Joshua Batson, and Christopher Olah. Sparse crosscoders for cross-layer features and model diffing. <https://transformer-circuits.pub/2024/crosscoders/>, 2024. Transformer Circuits Thread.

- [9] Julian Minder, Clément Dumas, Caden Juang, Bilal Chughtai, and Neel Nanda. Overcoming sparsity artifacts in crosscoders to interpret chat-tuning. *arXiv preprint arXiv:2504.02922*, 2025. doi: 10.48550/arXiv.2504.02922. URL <https://arxiv.org/abs/2504.02922>.
- [10] Niklas Muennighoff, Zitong Yang, Weijia Shi, Xiang Lisa Li, Li Fei-Fei, Hannaneh Hajishirzi, Luke Zettlemoyer, Percy Liang, Emmanuel Candès, and Tatsunori Hashimoto. s1: Simple test-time scaling. *arXiv preprint arXiv:2501.19393*, 2025. URL <https://arxiv.org/abs/2501.19393>.
- [11] Sagnik Mukherjee, Lifan Yuan, Dilek Hakkani-Tur, and Hao Peng. Reinforcement learning finetunes small subnetworks in large language models. *arXiv preprint arXiv:2505.11711*, 2025. doi: 10.48550/arXiv.2505.11711. URL <https://arxiv.org/abs/2505.11711>.
- [12] Constantin Venhoff, Iván Arcuschin, Philip Torr, Arthur Conmy, and Neel Nanda. Understanding reasoning in thinking language models via steering vectors. *arXiv preprint arXiv:2506.18167*, 2025. doi: 10.48550/arXiv.2506.18167. URL <https://arxiv.org/abs/2506.18167>. ICLR 2025 Workshop on Reasoning and Planning for LLMs (paper).
- [13] Jake Ward, Chuqiao Lin, Constantin Venhoff, and Neel Nanda. Reasoning-finetuning repurposes latent representations in base models. *arXiv preprint arXiv:2507.12638*, 2025. doi: 10.48550/arXiv.2507.12638. URL <https://arxiv.org/abs/2507.12638>. ICML 2025 Workshop on Actionable Interpretability.
- [14] Jason Wei, Xuezhi Wang, Dale Schuurmans, Maarten Bosma, Fei Xia, Ed H. Chi, Quoc V. Le, Denny Zhou, et al. Chain-of-thought prompting elicits reasoning in large language models. *arXiv preprint arXiv:2201.11903*, 2022. URL <https://arxiv.org/abs/2201.11903>.

A Appendix

A.1 Model Weights

Weights for the trained LoRA are available at <https://huggingface.co/jnward2/qwen-reasoning-lora>.

A.2 Selected LoRA Directions

We present a cherry-picked selection of interesting and interpretable LoRA directions, visualized with a dashboard. The full dashboard is available at https://jakeward.page/lora_sae_dashboard.html. On the left of the dashboard are max-activating examples of the direction over the training dataset. On the right, a full training sample is shown with activations highlighted. Highlight color represents whether the activation is positive or negative.

Layer 30 - up_proj (negative)

Analyzing top activating examples

Rollout 137, Example 1, Activation: -2.725

ten-element subset where each consecutive triplet satisfies $a_{i+2} \geq a_i + a_{i+1}$. But how does this relate to the actual numbers? Alternatively, maybe to ensure that in any ten-element subset, the three smallest

Rollout 485, Example 2, Activation: -2.689

$-10 = 49,990$? Wait, that can't be right. Wait: 0.1 divided by $2e-6$ is $0.1 / 0.0000$

Rollout 415, Example 3, Activation: -2.688

at C2. Wait, the correct structure for but-2-enoic acid is CH2CHCOOH. Wait, but that's only three carbons. No, but-2-enoic acid is: the carboxy

Rollout 861, Example 4, Activation: -2.686

$-x_B, p_A + p_B$ or $(x_A + x_B, p_A - p_B)$? Wait, in continuous-variable teleportation, the Bell measurement often measures $(x_A - x_B)$ and $(p_A +$

Full Context

Rollout 415

Threshold: 0.00 Intensity: 1.4x

Answer Choices:

(A) 0

(B) 8

(C) 3

(D) 4

Okay, let's see. The problem is about reaction steps and determining the number of distinct hydrogen signals in the ¹H NMR spectrum of the final product. The starting material is methyl (E)-but-2-enoate, which is then treated with a mixture of reagents to form product 1. Then product 1 is treated with excess methylmagnesium bromide to form product 2. They're asking how many chemically distinct non-exchanging hydrogen signals there are in the NMR of product 2.

First, I need to figure out what each reaction does. Let me start by drawing the structure of methyl (E)-but-2-enoate. That should be an ester, specifically the methyl ester of (E)-but-2-enoic acid. So the structure is CH3CH=CHCOOCH3. Wait, but-2-enoate: The double bond is between carbons 2 and 3. So the structure is CH2=CH-CO-CH3, and the E configuration means the higher priority groups on each carbon of the double bond are opposite. The COCH3 group is on one side, and the CH3 would be on the other. Wait, let me check: but-2-enoate is CH2-CO-CH=CH2? No, but-2-enoate would be the ester of but-2-enoic acid. But-2-enoic acid is CH2=CHCOOH, but with the double bond starting at C2. Wait, the correct structure for but-2-enoic acid is CH2=CHCOOH. Wait, but that's only three carbons. No, but-2-enoic acid is: the carboxylic acid group is on C1, then C2 and C3 are double bonded. So: CH2=CHCOOH. Wait, no. If it's but-2-enoic acid, the structure should be CH2=CH-CH2-COOH. So the double bond between C2 and C3, with COOH on C4. Wait, but-2-enoic acid has the double bond starting at C2, so the structure would be CH2=CHCOOH. Because but-2-enoic acid is CH2=CHCOOH, and then the ester would be CH2=CHCOOCH3. The methyl ester: So structure of methyl (E)-but-2-enoate is: the ester group is OCH3 attached to the carbonyl, which is attached to the double bond. The (E) configuration indicates that the groups on either side of the double bond that are highest priority are opposite. On the carbonyl side (left side), the groups are COCH3 and CH2OH. Wait, I might need to draw this properly.

Actually, methyl (E)-but-2-enoate should be: the ester group is OMe attached to the carbonyl, followed by a double bond between carbons 2 and 3 (but-2-enoate). So, let's number the carbons starting from the carbonyl group. The carbonyl is carbon 1. Then carbon 2 is double bonded to carbon 3. So the structure is Me-C(=O)-CH=CH2. Wait, but-2-enoate implies that the double bond is between carbons 2 and 3 of the butenoate chain. Wait, that's confusing. Let's get this straight: Let's consider the structure as follows: the carboxylic acid is but-2-enoic acid, which would be CH2=CHCOOH with the double bond at position 2. But but-2-enoic acid has four carbons with the double bond starting at C2, so the structure would be CH2=CHCOOH. Wait, no. If the COOH is carbon 1, then carbon 2 is adjacent, carbon 3, carbon 4. Therefore, but-2-enoic acid would be CH2=CHCOOH. Wait, no. If the COOH is on carbon 1, then but-2-enoic acid would have the double bond between carbons 2 and 3.

Figure 4: Autointerpretation: *Consistently activates on the token “Wait” (and surrounding commas/periods) across examples*

Layer 20 - up_proj (negative)

Analyzing top activating examples

Rollout 435, Example 1, Activation: -2.635

angle). For z to be a root of unity, it must satisfy $z^n = 1$, which implies that $r^n = 1$. Therefore, r must be 1 because the modulus of 1 is 1. Hence, any

Rollout 45, Example 2, Activation: -2.445

$(5m+1) - 4(m+1) \geq 0$. Calculate: $5m+1 - 4m - 4 = m - 3$. $m - 3 \geq 0 \implies m \geq 3$.

Rollout 300, Example 3, Activation: -2.410

$0 \leq \theta < 2\pi$, we define $S_n = r^{i\theta}$. For all positive reals S_n .

Rollout 778, Example 4, Activation: -2.373

$2000000 / 4^k$. Since $4^k = (2^2)^k = 2^{2k}$. Therefore, $2000000 / 4^k =$

Rollout 117, Example 5, Activation: -2.326

Full Context

Rollout 894

Threshold: 0.00 Intensity: 2.0x

For example, direct product of two fields with four elements, which has 4 elements, elements (0,0), (1,0), (0,1), (1,1). Multiplicatively, each non-zero element squared is (1,1) etc. But maybe for any n .

Wait, in F_4 , take element (1,1). Its multiplicative inverse is itself, since $(1,1) \cdot (1,1) = (1,1)$. (1,0) inverse is (1,0), etc. But in the product ring $F_2 \times F_2$, each non-zero element satisfies $x^2 = 1$, but according to the problem requirement, $x^{2m+1} = 1$.

Hold on. Take element (1,0) in $F_2 \times F_2$. Then, $(1,0)^{2m+1} = (1,0)$ since $(1,0)^2 = (1,0)$. But in the product, components compute componentwise. But in the component F_1 , the computation is within each field. However, in the product ring, $(1,0)^{2m+1} = (1,0)$. But problem states that we need $x^{2m+1} = 1$ (the additive identity), but in the product ring $(1,0)$ is not 1. Wait, no! Hold on. In the question state that $2m+1$ is odd. In the product ring, 1 is the multiplicative identity, which is (1,1). Hence, in the example of $F_2 \times F_2$, take element (1,0). Compute $(1,0)^{2m+1}$: it is $(1,0)$. In order to have an element x in the product ring such that $x^{2m+1} = 1$, every component must satisfy $x_i^{2m+1} = 1$.

Wait, in the product ring, each non-zero element must have each component a unit (either 1 in the field F_2 or 1 in F_4). Wait, so for instance, if the ring is a product ring like $F_2 \times F_4$, then a non-zero element would have, say, (1,0) where 0 is a non-zero. Then, raising this to the $(2m+1)$ th power gives (1,0). So depending on whether the exponent works in F_4 .

In F_4 , multiplicative order is 3, and we need $x^{2m+1} = 1$ where $2m+1$ is 3. Therefore, 3 divides $2m+1$.

$2m+1 \equiv 0 \pmod{3}$ happens when:

$2m+1 \equiv 0 \pmod{3} \implies 2m \equiv -1 \pmod{3} \implies 2m \equiv 2 \pmod{3} \implies m \equiv 1 \pmod{3}$. Since $2 \pmod{3} \cdot 2$ varies as 2, 1, 2, 1, ... per exponent parity. So $2m+1 \equiv 0 \pmod{3}$ when odd, $2m+1 \equiv 0 \pmod{3}$ when even. So $2m+1 \equiv 0 \pmod{3}$ if and only if m is odd. So if the ring has F_2 and F_4 as components, then $\text{mod} 3$ scenario, F_4 can be included as each non-zero element x satisfies $x^{2m+1} = 1$ since for $\text{mod} 3$, $2m+1 \equiv 0 \pmod{3}$ iff m is odd. Wait $\text{mod} 3$.

Wait, $m=1$, but the exponent is $2(1)+1=3$. Let me check for $m=1$, the exponent is 3, which agrees. Form 2: the exponent is 5, which would need to satisfy $x^5 = 1$ in F_4 , but multiplicative order in F_4 is 3, and $3 \nmid 5$. So $x^5 \neq 1$ in F_4 . But in multiplicative group F_4^* , which is cyclic of order 3, since 3 divides 5, hence $x^5 = x^2 = 1$ in F_4^* . Hence $x^5 = 1$ in F_4 , which implies $x=1$. But $x=1$ only for $x=1$. But there are elements where $x^2 = x+1$, which contradicts. Therefore, if the product ring includes fields other than F_2 as components, such as F_4 , then the order to satisfy $x^{2m+1} = 1$ in those fields require that the multiplicative exponents divide $2m+1$, which was discussed above for each.

Therefore, essentially, given a fixed n :

If n is odd, then to have F_4 in a product, we need that F_4 multiplicative order 3 divides $2m+1$. Since then $2m+1$ must be divisible by 3. When $2m+1$ is divisible by 3.

Figure 5: Autointerpretation: *single-letter math variables and exponent tokens*

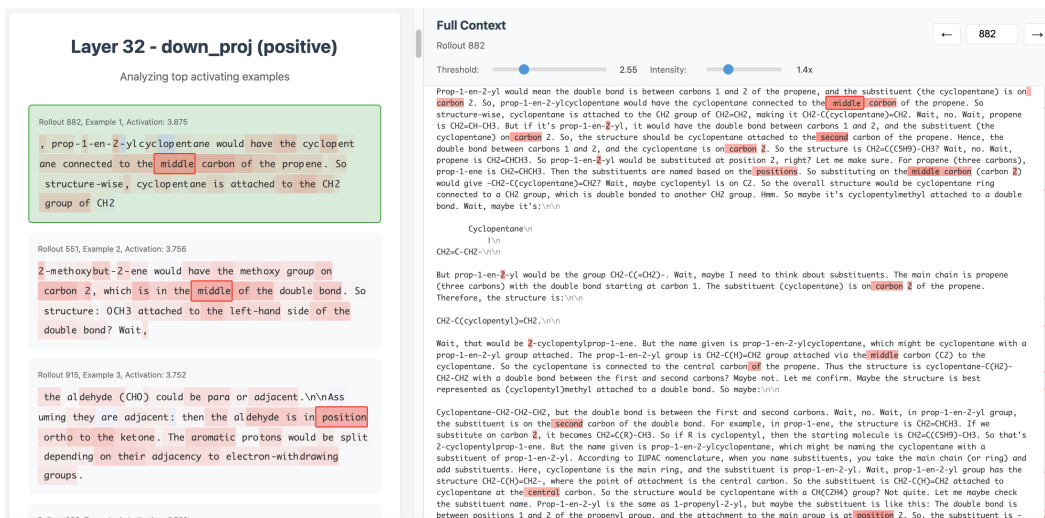


Figure 6: Autointerpretation: indicates positional numbering in molecules (position, numeral, middle)
Note: a thresholding operation was applied to make visualizing top activations in the full context easier.

A.3 Selected SAE Features

We additionally present a cherry-picked selection of SAE features. The dashboard screenshots highlight max-activating feature examples over the training dataset.

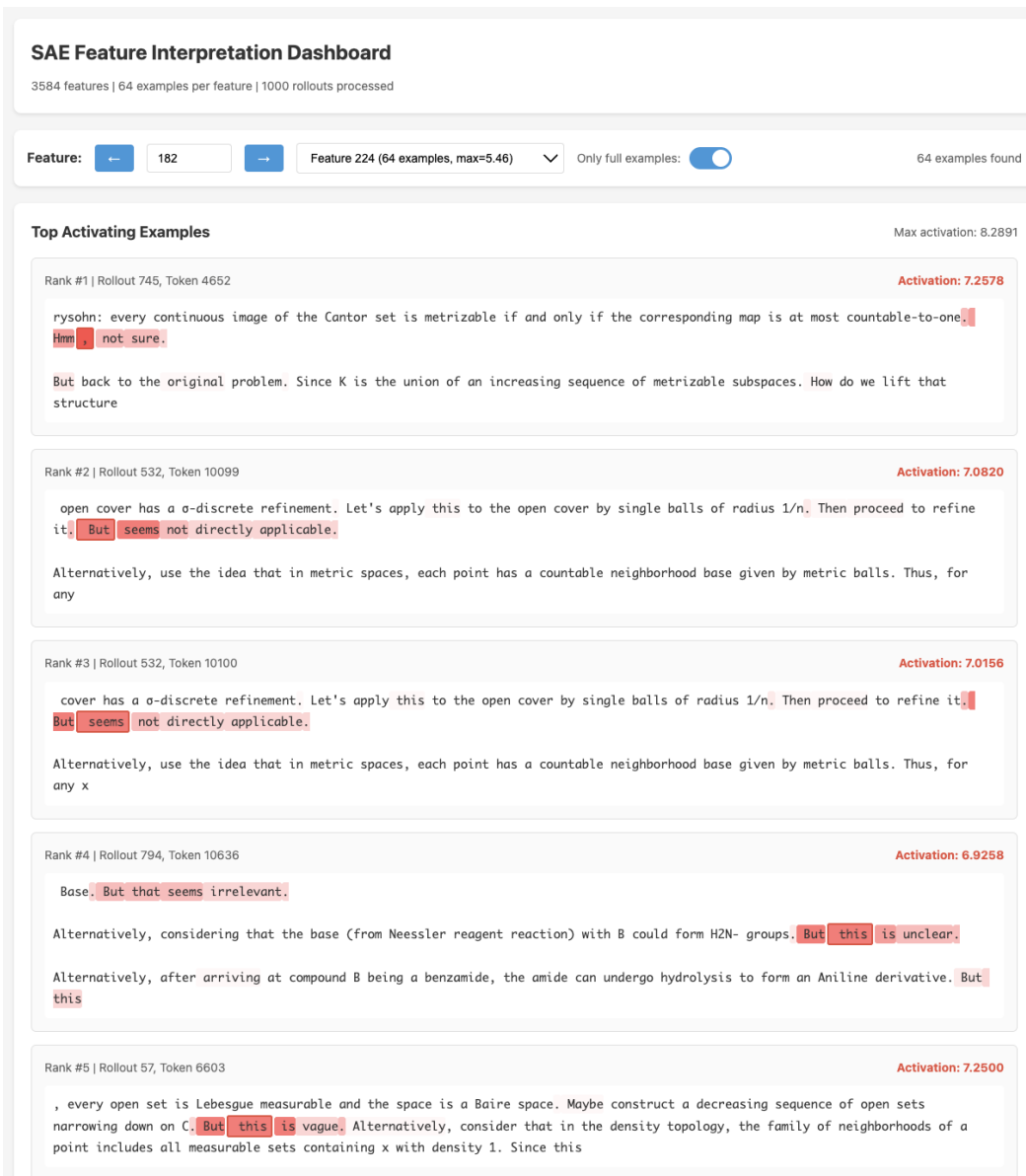


Figure 7: Autointerpretation: *Hesitation markers, notably “Hmm”, in reflective internal thought.*

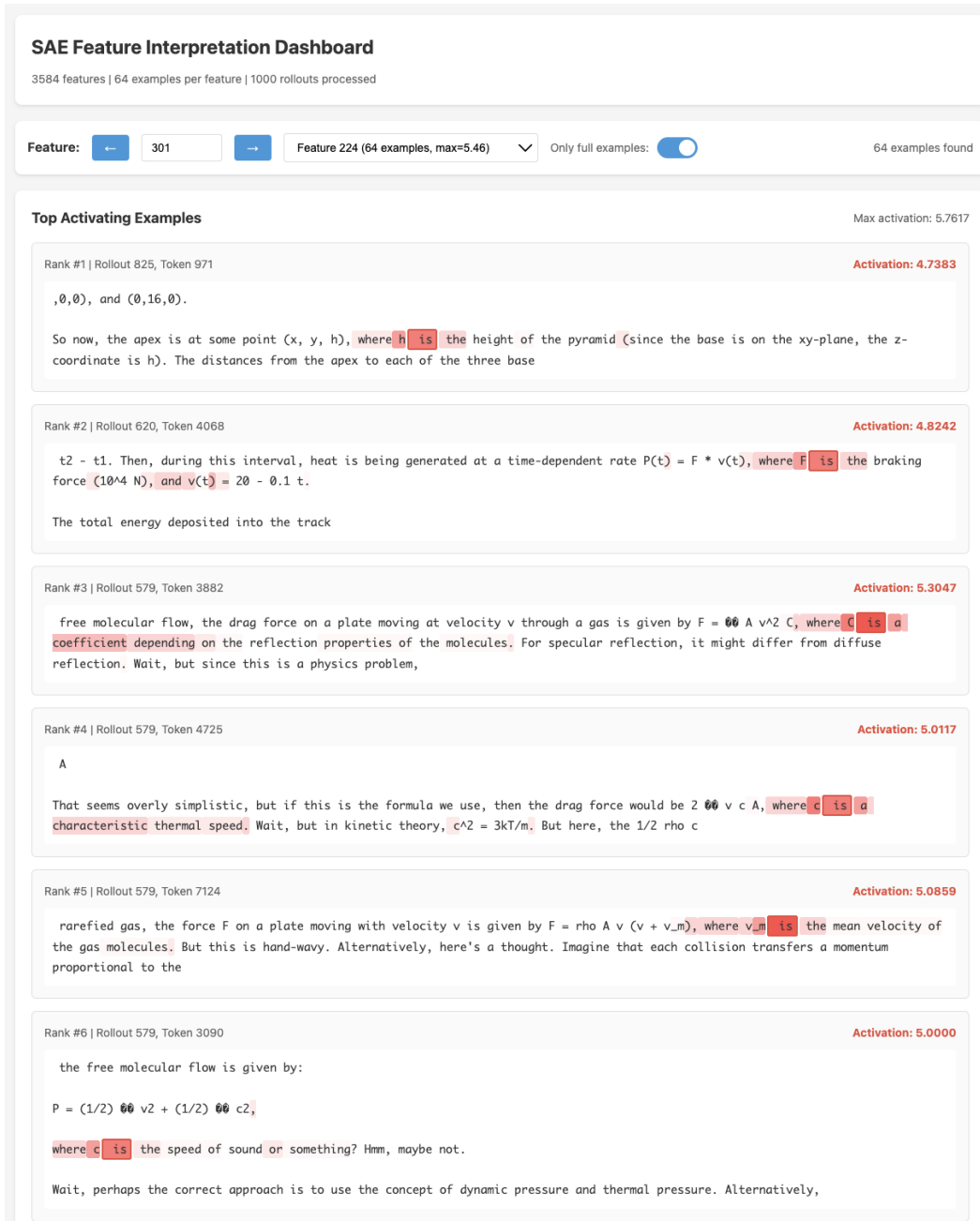


Figure 8: Autointerpretation: Firing on “is” as an equality indicator in mathematical definitions.

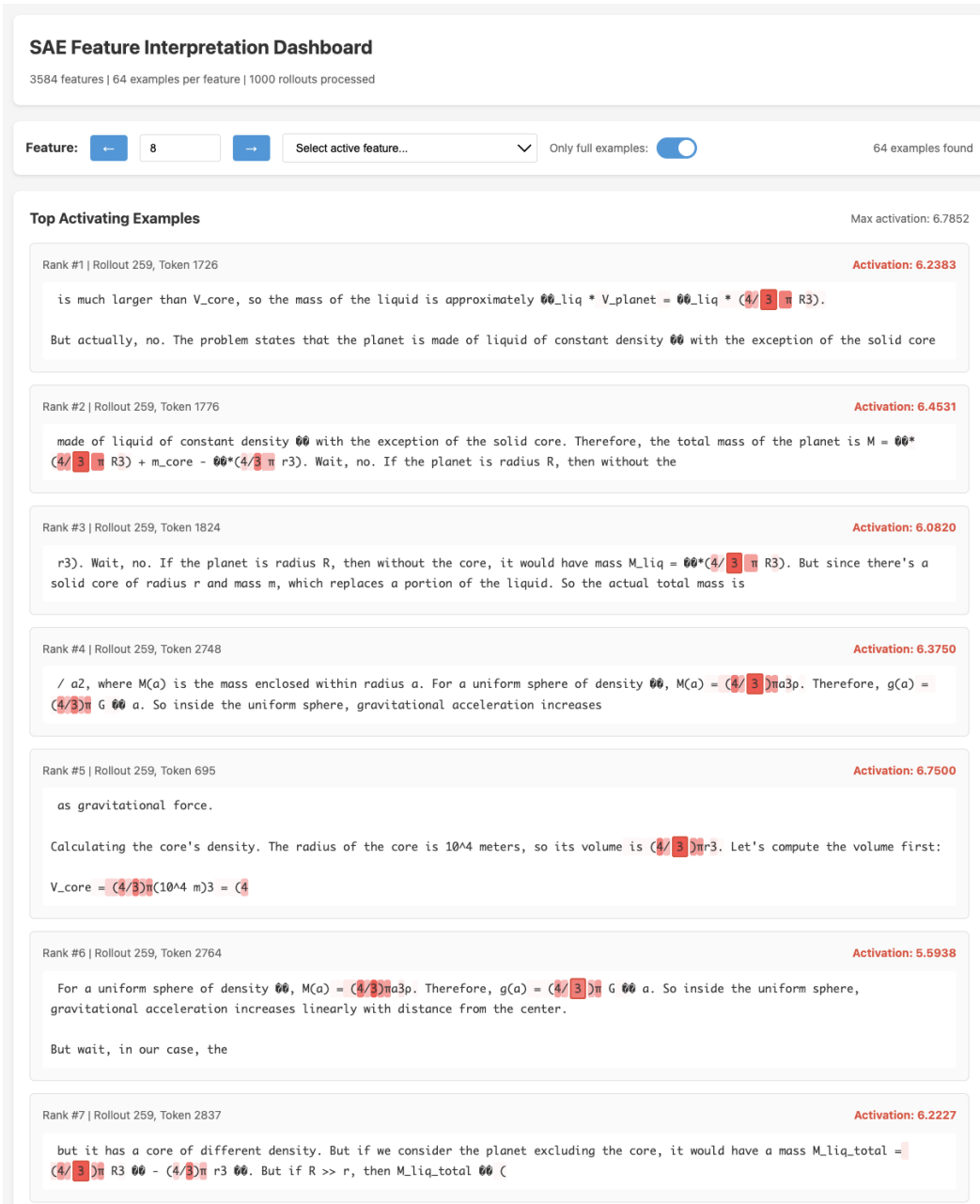


Figure 9: Autointerpretation: Sphere volume formula tokens, specifically $\frac{4}{3}\pi R^3$ components.

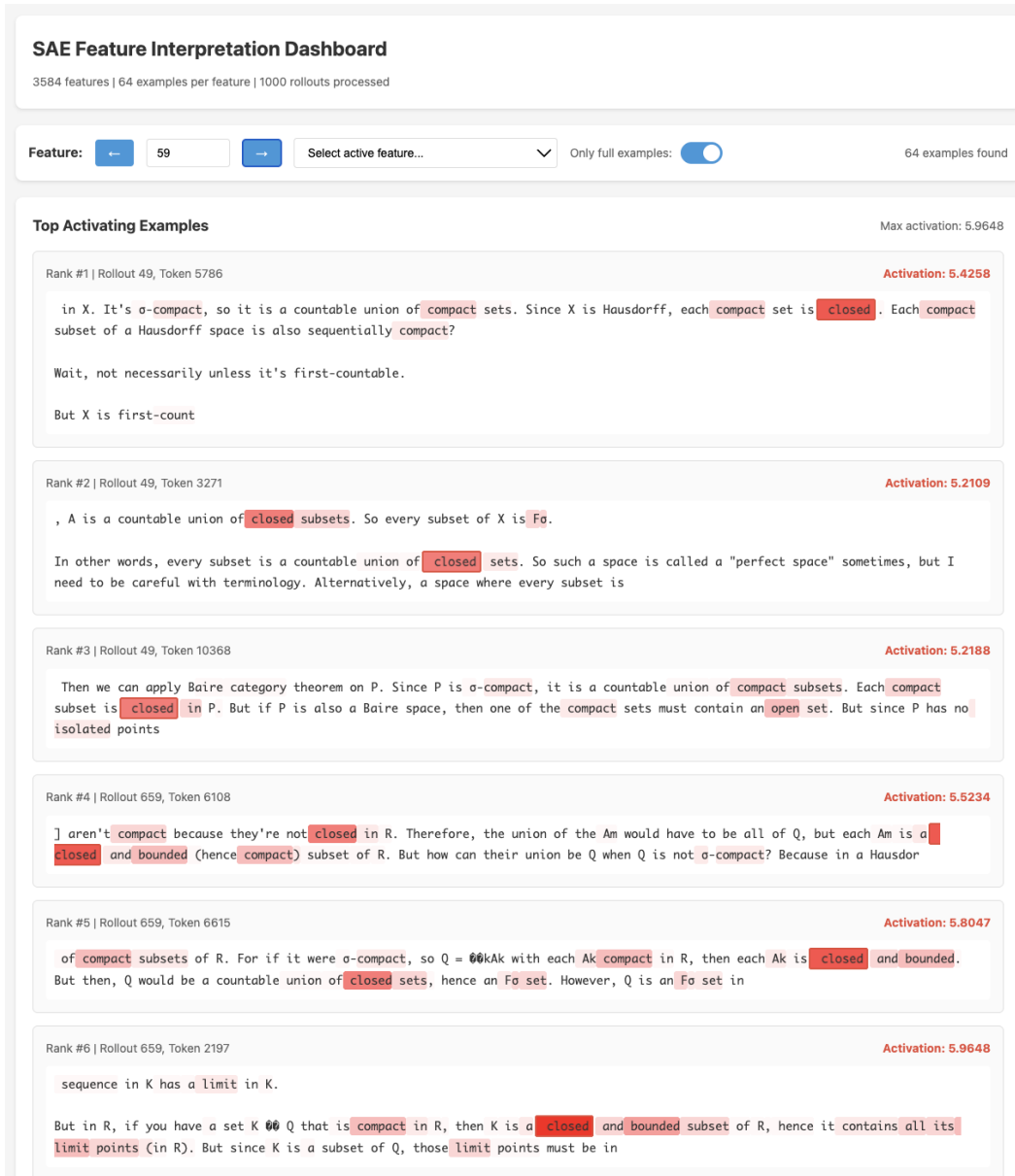


Figure 10: Autointerpretation: Fires on “closed” in mathematical topology contexts.

B LLM Prompts

B.1 Autointerpretation

We use gpt-5-mini to automatically generate interpretations for LoRA directions, MLP neurons, and SAE features:

We’re studying neurons in a neural network. Each neuron looks for some particular thing in a short document. Look at the parts of the document where the neuron activates and describe what it’s firing for.

Some activations will be noisy, in these cases you’ll have to look for common phrases or concepts in the examples.

If a feature always activates for the same token, you should note this in your \ explanation, and also state whether that feature represents that token in some \ specific context. You may need to look at words surrounding activating tokens \ in order to understand why a feature is firing. Features should have a clear, singular explanation and should be monosemantic. \ If there isn't a clear monosemantic explanation, note this.

Your explanation should not exceed ten words. Don't write complete sentences. \ The neuron might be responding to:

- Individual tokens or specific words
- Phrases or expressions
- Abstract concepts or behaviors
- Broader context or topics

The activation format shows the full text first, then lists tokens where the neuron \ fired along with their activation strengths (0-10 scale). Higher values mean \ stronger activation.

For example:
cat and mouse ran around the tree. They quickly
tree 7.81
ran 2.30
around 1.01

Look at every example, and then generate an explanation. After generating an \ explanation, assess how monosemantic the feature is.

```
<neuron_activations>
{activations_str}
</neuron_activations>
```

Classify the feature's interpretability:

0: The feature is specific, clear, and monosemantic. All given examples clearly \ adhere to the explanation. The explanation is not broad, and the examples are not \ noisy. This feature has a clear and obvious interpretation.
1: The feature may be broad or noisy, but ALL given examples still adhere to the \ generated explanation. The explanation may not be obvious.
2: The feature appears polysemantic. Some examples do not clearly adhere to the \ generated explanation. The explanation does not clearly explain the given examples.

Respond with JSON in exactly this format:

```
{
  "explanation": "your concise explanation in just a few words",
  "classification": <0, 1, or 2>,
  "classification_reasoning": "brief justification for your classification"
}
```

B.2 Autocategorization

We use claude-opus-4.1 to generate feature categories given feature interpretations using the following prompt:

You will be provided with a list of interpretations of MLP neurons from a \ large language model. Each interpretation describes what a particular learned \ feature detects or responds to during tasks. Your task is to identify high-level functional role categories that capture what \ these features are doing computationally.

Read through all feature interpretations carefully
Identify natural groupings based on the computational or functional role each \ feature plays
Generate 5-8 high-level categories that capture the major functional roles

Important considerations:

- Focus on computational function (what role the feature plays) rather than \ surface-level similarity
- Categories should be mutually exclusive when possible, though some features \ may have dual roles
- Aim for categories that would generalize across different types of tasks
- Include 3-5 example feature interpretations for each category (copied exactly \ from the list provided)

Output your response as a JSON object with the following structure:

```
““json
{
  "categories": [
    {
      "string_id": "category_identifier_in_snake_case",
      "name": "Human Readable Category Name",
      "definition": "A 1-2 sentence description of what functional role these features serve.",
      "examples": [
        "exact feature interpretation from the list",
        "another feature interpretation from the list",
        "additional examples as needed"
      ]
    }
  ],
  "summary": "Your overall categorization logic and any notable patterns you observed"
}
““
```

Ensure your response contains ONLY the JSON object, with no additional text before or after.

Here are the feature interpretations to categorize:

{feature_list}

Given these categories, we categorize each feature using gpt-5-mini using the following prompt:

Categorize this neural network feature into ONE of the given categories.

Feature explanation: "{feature.explanation}"

Activation examples (showing what tokens/contexts activate this feature):

{examples_str}

Available categories:

{categories_str}

Based on the feature explanation and activation examples, which category best fits this feature?
Reply with ONLY the category string_id, nothing else.

Your response:

C Additional Data

Task	Full LoRA	Full LoRA (attn-ablated)	Full LoRA (mlp-ablated)
AIME'24 (no-figures)	0.5000 (100.00%)	0.3667 (50.02%)	0.1333 (-37.50%)
MATH500	0.9100 (100.00%)	0.9000 (86.84%)	0.8440 (13.16%)
GPQA-Diamond	0.5808 (100.00%)	0.5152 (27.83%)	0.5051 (16.72%)

Table 2: Absolute scores with percentages in parentheses, computed relative to the Full Rank-1 LoRA’s recovered gain: $(x - b)/(\ell - b) \times 100\%$, where b is the baseline and ℓ is the Full LoRA score (so Full LoRA is 100%).